

Structural evidence against current induced destruction of the long-range charge ordering in manganese oxides

A. Wahl, V. Caignaert, S. Mercone

*Laboratoire CRISMAT, UMR 6508, ENSICAEN - Université de Caen,
6 Boulevard du Maréchal Juin, 14050 Caen Cedex, France.*

F. Fauth

*European Synchrotron Radiation Facility (ESRF)
6, Rue Jules Horowitz, F-38043 Grenoble, France*

(June 24, 2003)

Abstract

High-resolution synchrotron powder diffraction, in the presence of an applied current, has been used for studying the stability *upon current biasing* of the charge ordered phase in the manganese oxides $\text{Nd}_{0.6}\text{Ca}_{0.4}\text{MnO}_3$ and $\text{Pr}_{0.63}\text{Ca}_{0.37}\text{MnO}_3$. We demonstrate that the charge ordered structure is unchanged when a current ($I_{max} = 10\text{mA}$) is flowing through the sample. Such a result clearly indicates that the non-linear conduction observed in charge ordered manganites can not be ascribed to a current-induced destabilization of the long-range charge ordering.

Typeset using REVTeX

Rare earth manganites with general chemical formula $R_{1-x}A_x\text{MnO}_3$ (R and A are trivalent rare-earth and divalent ions, respectively) show a wide variety of electronic and magnetic properties such as colossal magnetoresistance, $\text{Mn}^{3+}/\text{Mn}^{4+}$ charge ordering (CO) and/or orbital ordering (OO).¹⁻³ The physics of the destabilization of the CO by different types of external perturbation has recently been under very active investigation.⁴⁻¹¹ So far, it is well established that the CO is stabilized by lattice distortions. Thus, a change of this distortion by tuning the average-A-site cationic radius can alternatively weaken or reinforce the CO.¹² Besides, it has been reported that irradiation by X-rays⁶ or light¹¹ and application of pressure⁷⁻⁹ or magnetic field⁵ can also induce a melting of the CO, leading to a transition from a charge-localized (CL) to a charge-delocalized state (CD). Application of an electric field is also known to induce a CL-CD transformation ; this latter feature is always associated with a strong non-linearity of the tension-current characteristics (V-I).^{10,13-16}

Up to now, it is not clear whether the underlying mechanism at the origin of this transition is the same for all perturbations, in particular for the electric field induced transition. In the latter case, this feature is interpreted in terms of current induced destabilization of the long-range CO state leading to the creation of conducting paths along the current flow.^{10,13-16} Recent experimental results do not agree with such a current-induced CO melting scenario. Indeed, electrical measurements, performed on the ferromagnetic non-charge ordered compound $\text{Pr}_{0.8}\text{Ca}_{0.2}\text{MnO}_3$, also exhibit a current induced CL-CD transition associated with a strong non linearity of the V-I characteristics.¹⁷ In such a case, the destruction of the CO can not be invoked, suggesting that the mechanism is more complex than the one initially proposed. In this paper, we present an alternative way to reinforce this hypothesis, consisting in measuring the crystal structure of a typical charge ordered material under application of an electric current.

The antiferromagnetic manganites $\text{Pr}_{0.63}\text{Ca}_{0.37}\text{MnO}_3$ and $\text{Nd}_{0.6}\text{Ca}_{0.4}\text{MnO}_3$ have been measured by synchrotron powder diffraction (SPD) techniques. Details for synthesis of the samples are reported elsewhere.¹⁸ Measurements have been performed as a function of both temperature (100-295K) *and current* (0-10mA) on the high-resolution powder diffrac-

tion beamline ID31 at ESRF (Grenoble, France) using an incident wavelength of 0.413 Å. The samples appeared as rods of compacted powders whose typical sizes ($1 \times 2 \times 3 \text{ mm}^3$) allowed an homogeneous sample cooling together with a suitable beam transmission. Improved powder averaging was achieved by oscillating the sample. Two indium contacts were soldered onto the $1 \times 2 \text{ mm}^2$ section of the sample, leaving an uncovered $2 \times 3 \text{ mm}^2$ section facing the synchrotron beam of $0.8 \times 1.5 \text{ mm}^2$ size. V-I data were taken with current biasing using a Keithley 236. In addition to patterns collected on the compacted powder samples, data acquisition was also performed in the usual way (fine powder of the same compounds enclosed in 0.5mm diameter spinning capillaries). In this latter case, the better powder averaging considerably increases the statistics and thus the accuracy in structure determination. All our X-rays diffraction patterns have been analyzed using the Rietveld method.

At room temperature, both compounds display the commonly observed double perovskite structure with orthorhombic cell, $a \simeq a_p\sqrt{2}$, $b \simeq 2a_p$, $c \simeq a_p\sqrt{2}$ and $Pnma$ space group (here, a_p denotes the perovskite lattice parameter). At 100K, both compounds exhibit ($h/2, k, l$)-type superstructure peaks induced by the unit cell doubling along the a -axis (see figure 1). Such a crystallographic phase transition is associated to the long-range ordering of the Mn^{3+} and Mn^{4+} species occurring in $R_{1-x}A_x\text{MnO}_3$ -type manganites.¹⁹⁻²¹ From both temperature dependent data collection and *in situ* resistivity measurements, we precisely determined the charge ordering temperatures $T_{CO}=235\text{K}$ and 240K for $\text{Pr}_{0.63}\text{Ca}_{0.37}\text{MnO}_3$ and $\text{Nd}_{0.6}\text{Ca}_{0.4}\text{MnO}_3$, respectively. Refinements of the CO phase were performed according to the constraint model initially proposed by Radaelli *et al.* for $\text{La}_{0.5}\text{Ca}_{0.5}\text{MnO}_3$ ²⁰.

High resolution X-ray scattering measurements in the presence of an applied direct current would permit to determine unambiguously whether the current induced CL-CD transition associated with the non-linear V-I characteristics can be linked to a destruction of the long-range CO. A strong non-linearity i.e. a deviation from the Ohm's law, is observed when the bias current attains a threshold value for $\text{Pr}_{0.63}\text{Ca}_{0.37}\text{MnO}_3$ and $\text{Nd}_{0.6}\text{Ca}_{0.4}\text{MnO}_3$. This non-linearity is even more obvious when $\frac{R}{R_{ohmic}}$ vs I curves are plotted ($R_{ohmic} = R(I \rightarrow 0)$) (See figure 2a and 2b). As expected the resistance is independent of the bias current in

the ohmic regime and strongly decreases above a critical current value.²² Looking at figure 2, a rough estimate for the critical values of the current gives $I_c = 4$ mA and 2 mA for $\text{Pr}_{0.63}\text{Ca}_{0.37}\text{MnO}_3$ and $\text{Nd}_{0.6}\text{Ca}_{0.4}\text{MnO}_3$, respectively.

So far, we have evidenced for both samples the onset of a single long-range CO phase at 100K as well as a deviation of the ohm's law above a given applied current. In order to unambiguously determine whether the non-linear conduction above I_c is related with any complete or partial CO melting process, we have collected SPD data under application of an electric current up to 10 mA. Whatever the applied current, the CO phase remains unchanged as can be seen from the constant behavior of the CO superstructure peaks intensity (see Insets of figure 2) and/or width (see figure 3).

Moreover, for $T < T_{CO}$, it is worth noting that a comparison of the current *and* thermal dependence of the unit cell volume, rules out any Joule heating effect in our data acquisition procedure (See figure 4 for $\text{Nd}_{0.6}\text{Ca}_{0.4}\text{MnO}_3$). Indeed, no evolution of the unit cell volume is observed as a function of the applied current ($I_{\text{max}} = 10$ mA, well above I_c) whereas, in the range of temperature above 100K, a steep increase is observed with zero biased current.

Our SPD results do not give a direct interpretation of the non-linear conduction effects, but at least, discard any destabilization of the long- range CO as the origin for this feature. Other interpretations, based on a preserved superstructure when a current is flowing, should now be proposed. The system behaves in such a way that the bias current may generate metallic path giving rise to resistivity drop. One can describe this feature by considering coexistence of localized and delocalized electron states with independent path of conduction. This situation is analog to what occurs in charge density waves systems.²⁴ In charge ordered compounds, observation of non-linear conduction setting in along with a large broad band noise suggests that the charge ordered state gets depinned at the onset of the non-linear regime.^{23,15} Besides, the possibility of a charge density wave (CDW) condensate in this charge ordered regime of the manganese oxides is now well established.²⁵⁻²⁷ Recently, we have proposed an analogy with CDW systems has been proposed.²² The non-linear transport

properties are explained by the motion of charge density waves, which carry a net electrical current, superimposed to the poorly mobile carriers of the system, when the current reaches a critical current necessary to overcome the pinning forces acting on the CDW condensate.

In conclusion, the stability of the charge ordering upon current biasing has been studied for compounds $\text{Pr}_{0.63}\text{Ca}_{0.37}\text{MnO}_3$ and $\text{Nd}_{0.6}\text{Ca}_{0.4}\text{MnO}_3$. High resolution X-ray diffraction patterns have been collected simultaneously with electrical measurements. It is shown that, despite the occurrence of a strong non linear conduction, the superstructure peaks associated to the long-range ordering of the Mn^{3+} and Mn^{4+} species are not modified by current biasing. This implies that the long-range charge ordering in manganites is not destroyed when a current is flowing in the sample.

REFERENCES

- ¹ E. O. Wollan and W. C. Koehler, Phys. Rev. **100**, 545 (1955); J. B. Goodenough, *ibid.* **100**, 564 (1955).
- ² For a review, see *Colossal Magnetoresistance, Charge Ordering and Related Properties of Manganese Oxides*, edited by C. N. R. Rao and B. Raveau (World Scientific, Singapore, 1998) and *Colossal Magnetoresistive Oxides*, edited by Y. Tokura (Gordon and Breach Science, New York).
- ³ S. Jin, T. H. Tiefel, M. McCormack, R. A. Fastnacht, R. Ramesh, and L. H. Chen, Science **264**, 413 (1994); R. von Helmolt, J. Wecker, B. Holzapfel, L. Schultz, and K. Samwer, Phys. Rev. Lett. **71**, 2331 (1993).
- ⁴ M. R. Lees, J. Barratt, G. Balakrishnan, D. McK. Paul, and M. Yethiraj, Phys. Rev. B. **52**, R14 303 (1995).
- ⁵ Y. Tomioka, A. Asamitsu, Y. Moritomo, and Y. Tokura, J. Phys. Soc. Jpn. **64**, 3626 (1995).
- ⁶ V. Kiryukhin, D. Casa, J. P. Hill, B. Keimer, A. Vigliante, Y. Tomioka, and Y. Tokura, Nature (London) **386**, 813 (1997).
- ⁷ M. Fiebig, K. Miyano, Y. Tomioka and Y. Tokura, Science **280**, 1925 (1998).
- ⁸ K. Ogawa, W. Wei, K. Miyano, Y. Tomioka and Y. Tokura, Phys. Rev. B **57**, R15033 (1998)..
- ⁹ Y. Moritomo, H. Kuwahara, Y. Tomioka and Y. Tokura, Phys. Rev. B **55**, 7549 (1997).
- ¹⁰ A. Guha, A. Raychaudhuri, A. Raju and C. N. R. Rao, Phys. Rev. B **62**,5320 (2000)
- ¹¹ K. Miyano, T. tanaka, Y. Tomioka and Y. Tokura, Phys. Rev. Lett. **78**, 42 57 (1997)
- ¹² C. Martin, A. Maignan, M. Hervieu, and B. Raveau, Phys. Rev. B **60**, 12 191 (1999).

- ¹³ A. Asamitsu *et al.*, Nature **388**, 50 (1997).
- ¹⁴ A. Guha, N. Khare, A. Raychaudhuri and C. N. R. Rao, Phys. Rev. B **62**,R11941 (2000)
- ¹⁵ C. N. R. Rao, A. Raju, V. Ponnambalam, S. Parashar and N. Kumar, Phys. Rev. B **61**, 594 (2000)
- ¹⁶ R. C. Budhani, N. K. Pandey, P. Padhan, S. Srivastava and R. P. S. M. Lobo, Phys. Rev. B **65**, 014429 (2001)
- ¹⁷ S. Mercone, A. Wahl, Ch. Simon and C. Martin, Phys. Rev. B **65**, 214428 (2002).
- ¹⁸ A. Maignan, C. Martin, F. Damay, and B. Raveau, Z. Phys. B **104**, 21 (1997).
- ¹⁹ Z. Jiráček, S. Krupička, Z. Šimša, M. Dlouhá, and S. Vratislav, J. Magn. Magn. Mater. **53**, 153 (1985).
- ²⁰ : P. G. Radaelli, D. E. Cox, M. Marezio, and SW. Cheong, Phys. Rev. B **55**, 3015 (1997)
- ²¹ D. E. Cox, P. G. Radaelli, M. Marezio and S-W. Cheong, Phys. Rev. B **57** 3305 (1998).
- ²² A. Wahl, S. Mercone, A. Pautrat, M. Pollet, Ch. Simon, cond-mat. 0306161
- ²³ A. Guha, A. Gosh, A. Raychaudhuri, S. Parashar, A. Raju and C. N. R. Rao, App. Phys. Lett. **75** 3381 (1999)
- ²⁴ G. Grüner, Rev. Mod. Phys. **60**, 1129 (1988) and references therein.
- ²⁵ N. Kida and M. Tonouchi, Phys. Rev. B **66**, 024401 (2002).
- ²⁶ Y. D Chuang, A. D. Gromko, D. S. Dessau, T. Kimura and Y. Tokura, Science **292**, 1509 (2001)
- ²⁷ T. Asaka, S. Yamada, S. Tsutsumi, C. Tsuruta, K. Kimoto, T. Arima and Y. Matsui, Phys. Rev. Lett. **88**, 097201 (2002)

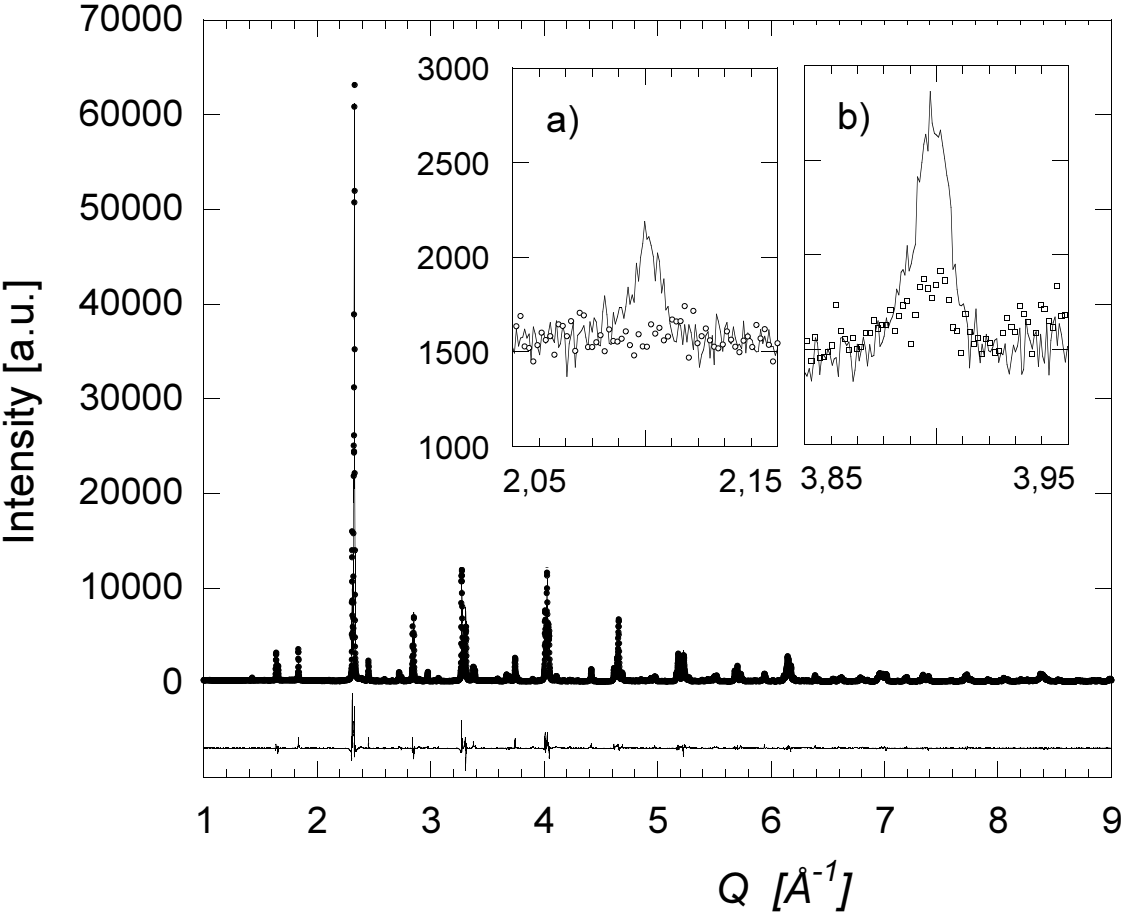
I. FIGURES CAPTIONS

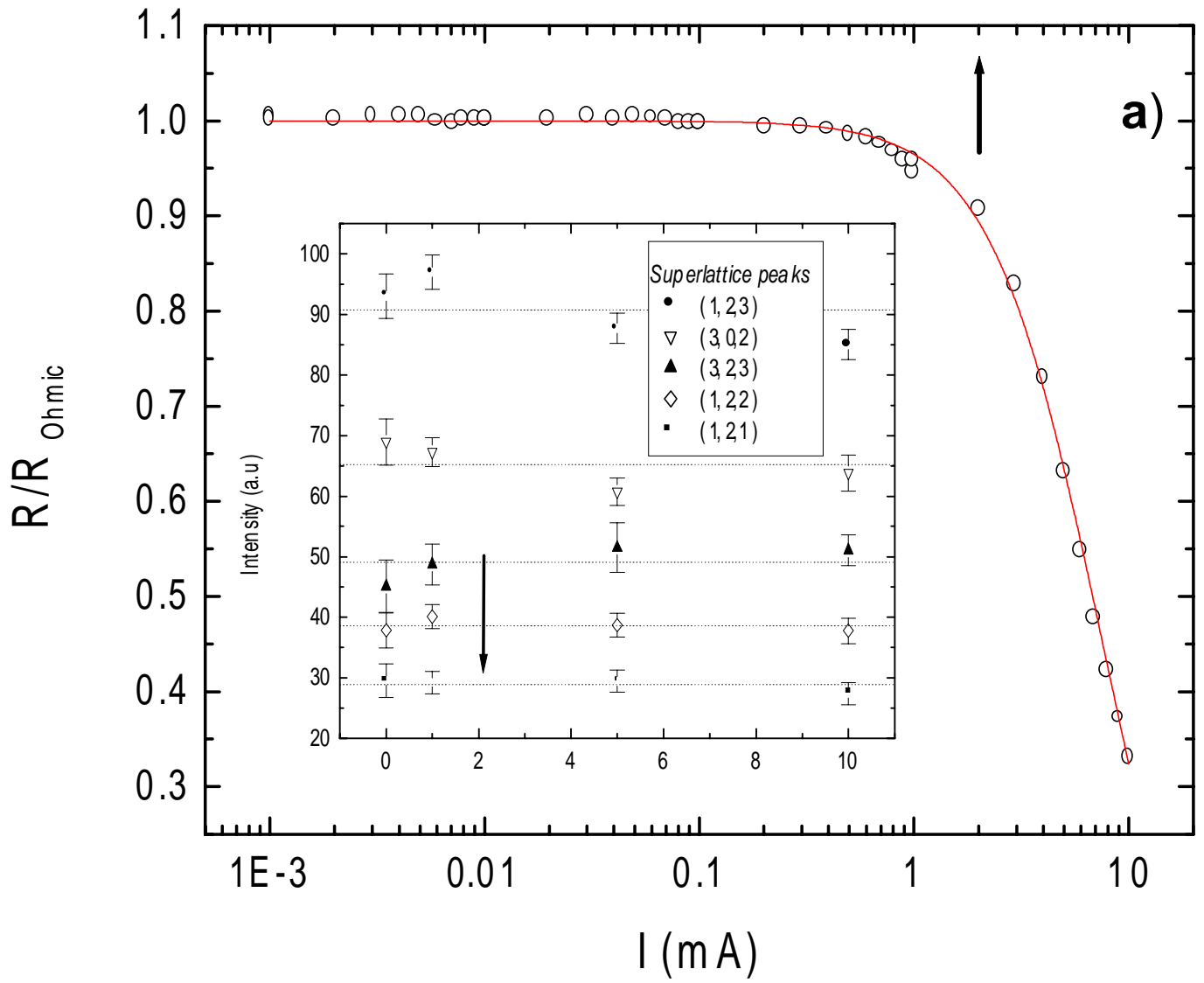
Figure 1 : Observed, calculated and difference patterns of $\text{Nd}_{0.6}\text{Ca}_{0.4}\text{MnO}_3$ at 100K with zero bias. Here, SPD data were collected on powder capillary. Inset : (121) (a) and (123) (b) CO superstructure peak region measured at 100K (solid line) and 295K (symbols) on a compacted powder of the same compounds.

Figure 2 : $\frac{R}{R_{Ohmic}}$ versus bias current at 100K for $\text{Nd}_{0.6}\text{Ca}_{0.4}\text{MnO}_3$ (a) and $\text{Pr}_{0.63}\text{Ca}_{0.37}\text{MnO}_3$ (b). The arrow denotes the estimated threshold current. Insets : Integrated intensity of the superlattice peaks as a function of the bias current at 100K. The arrows denote the occurrence of the non-linear regime.

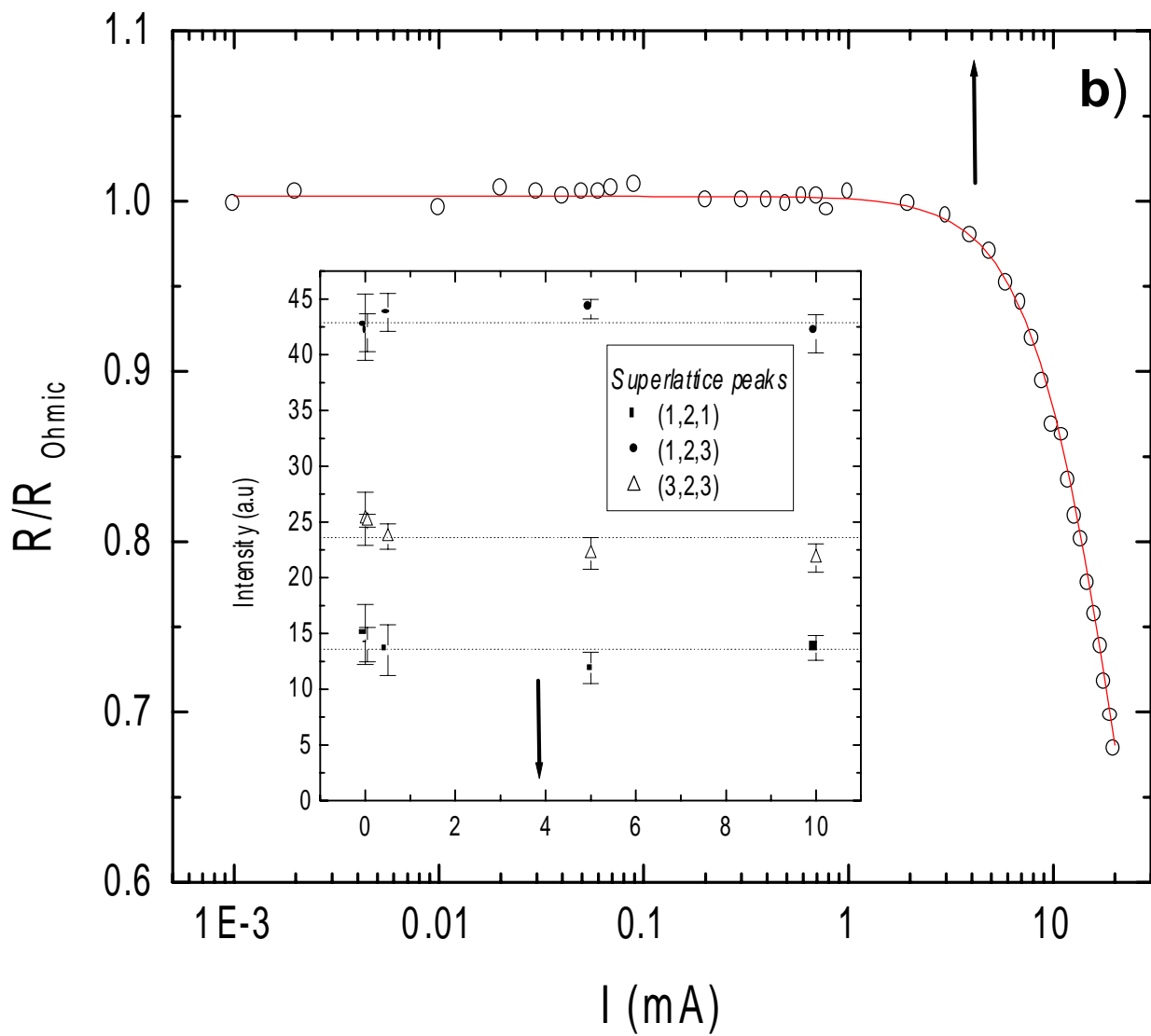
Figure 3 : Portion of the x-ray diffraction patterns for $\text{Nd}_{0.6}\text{Ca}_{0.4}\text{MnO}_3$ at 100K with bias 0 mA, 1 mA and 5 mA in the region of the (123) superlattice peak.

Figure 4 : Cell volume versus temperature for zero bias (filled symbol, lower scale) and cell volume versus bias current at 100K (upper scale)





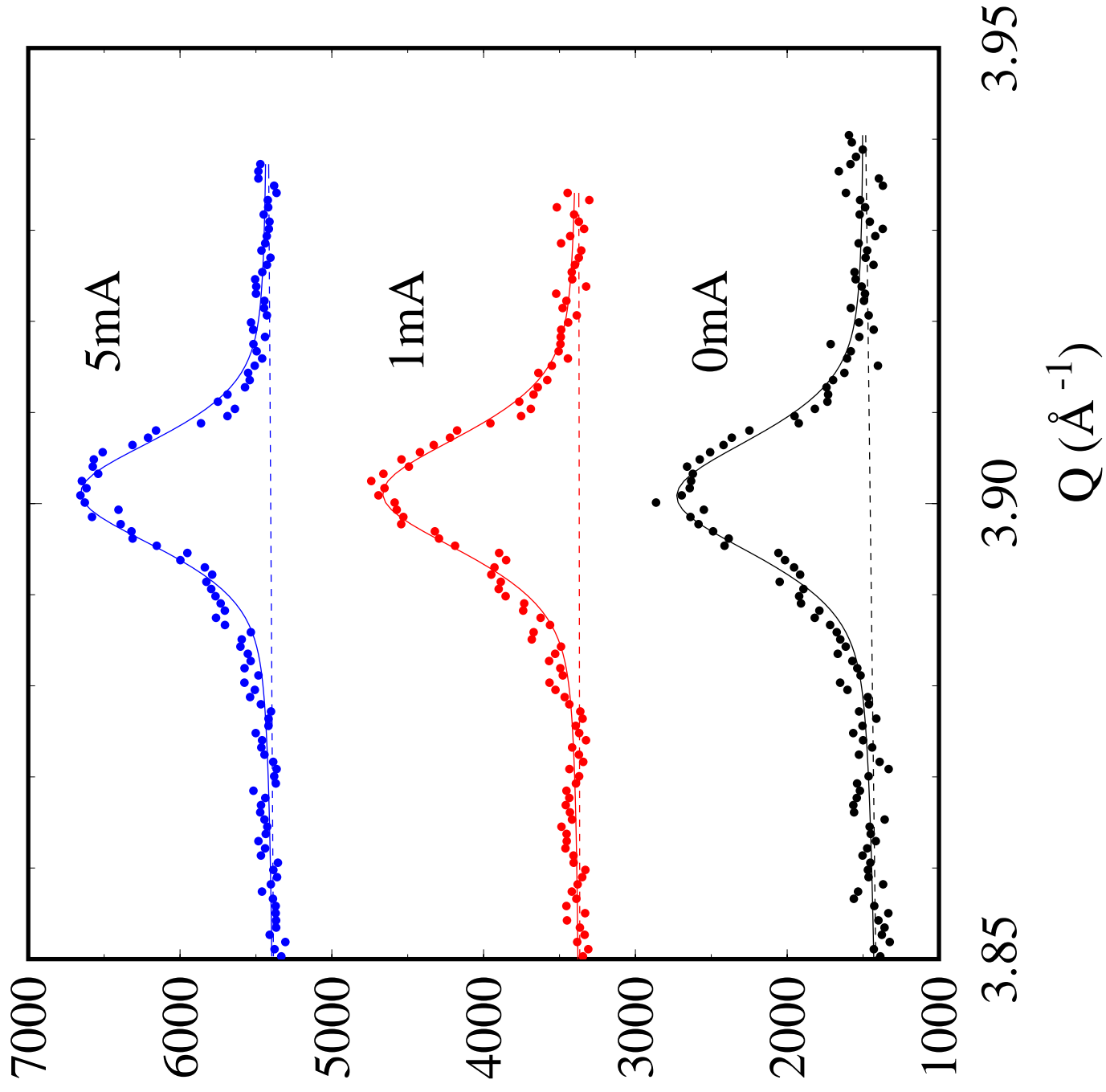
Physical Review B
 A. Wahl et al.
Figure 2a

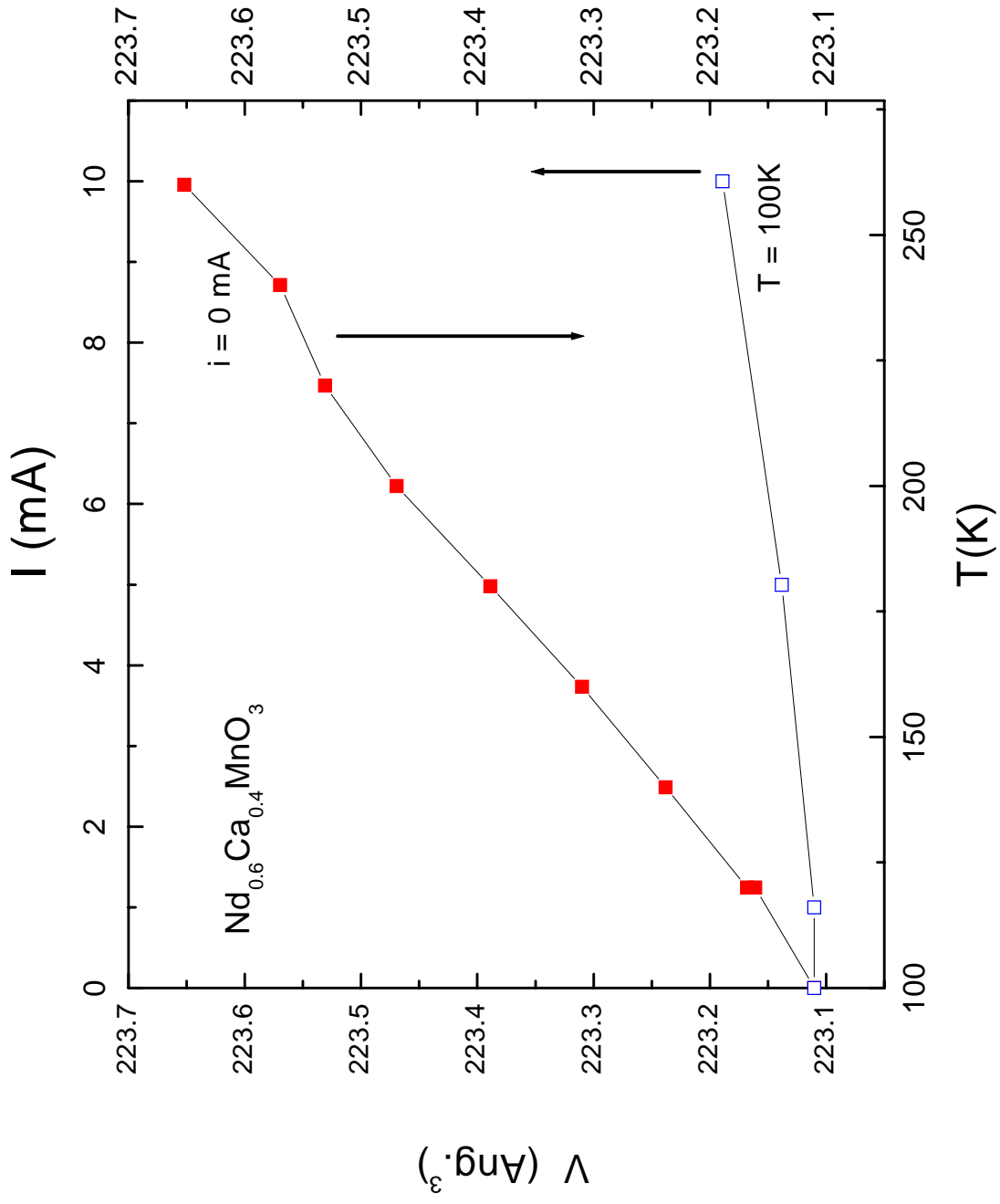


Physical Review B

A. Wahl et al.

Figure 2b





Physical Review B

A. Wahl et al.

Figure 4